Magnetocaloric effect in Fe$_2$P: Magnetic and phonon degrees of freedom

J. Cedervall,[1,*] M. S. Andersson,[2,3] E. K. Delczeg-Czirjak,[4] D. Iuşan,[4] M. Pereiro,[4] P. Roy,[5] T. Ericsson,[6] L. Häggström,[6] W. Lohstroh,[7] H. Mutka,[8] M. Sahlberg,[1] P. Nordblad,[2] and P. P. Deen[9,10,†]

[1]*Department of Chemistry - Ångström Laboratory, Uppsala University, Box 538, SE-751 21 Uppsala, Sweden*
[2]*Department of Engineering Sciences, Uppsala University, Box 534, SE-751 21 Uppsala, Sweden*
[3]*Department of Chemistry and Chemical Engineering, Chalmers University of Technology, Göteborg SE-412 96, Sweden*
[4]*Division of Materials Theory, Department of Physics and Astronomy, Uppsala University, Box 516, SE-751 20 Uppsala, Sweden*
[5]*Institute for Molecules and Materials, Radboud University Nijmegen, Heyendaalseweg 135, 6525 AJ, Nijmegen, The Netherlands*
[6]*Department of Physics and Astronomy, Uppsala University, Box 516, SE-751 20 Uppsala, Sweden*
[7]*Technische Universität München, Garching bei München, Heinz Maier-Leibnitz Zentrum (MLZ),
Lichtenbergstrasse 185748 Garching, Germany*
[8]*Institut Laue-Langevin, B.P. 156, 38042 Grenoble Cedex 9, France*
[9]*European Spallation Source ESS ERIC, Box 176, SE-221 00 Lund, Sweden*
[10]*Nanoscience Center, Niels Bohr Institute, University of Copenhagen, DK-2100 Copenhagen Ø, Denmark*

Devices based on magnetocaloric materials provide great hope for environmentally friendly and energy efficient cooling that does not rely on the use of harmful gasses. Fe$_2$P based compounds are alloys that have shown great potential for magnetocaloric devices. The magnetic behavior in Fe$_2$P is characterized by a strong magnetocaloric effect that coexists with a first-order magnetic transition (FOMT). Neutron diffraction and inelastic scattering, Mössbauer spectroscopy, and first-principles calculations have been used to determine the structural and magnetic state of Fe$_2$P around the FOMT. The results reveal that ferromagnetic moments in the ordered phase are perturbed at the FOMT such that the moments cant away from the principle direction within a small temperature region. The acoustic-phonon modes reveal a temperature-dependent nonzero energy gap in the magnetically ordered phase that falls to zero at the FOMT. The interplay between the FOMT and the phonon energy gap indicates hybridization between magnetic modes strongly affected by spin-orbit coupling and phonon modes leading to magnon-phonon quasiparticles that drive the magnetocaloric effect.

I. INTRODUCTION

Magnetic refrigeration is based on the magnetocaloric effect (MCE) in which a magnetic material is cooled upon adiabatic demagnetization with a magnetic entropy change. This technique will yield a safer and more energy efficient device compared to conventional gas compression refrigerators [1–4]. Optimal working conditions are achieved for compounds with large changes in entropy (ΔS). This is typically achieved in ferromagnetic materials with a ferromagnetic to paramagnetic transition temperature (T_c) close to the operating temperature since the entropy change is largest at T_c. ΔS is associated with internal degrees of freedom that include phonon modes, spin waves, and phonon-electron interactions. Understanding the interplay between spin, electron, and lattice degrees of freedom is essential to optimize MC devices. Even though the MCE was first observed in 1881 [5], there remains little understanding of the interactions between these degrees of freedom. Today, a large number of MCE materials exist [6,7]. One class of materials that has been thoroughly studied is based on the hexagonal compound Fe$_2$P, which exhibits a first-order magnetic phase transition (FOMT) with strong magnetic anisotropy and magnetoelastic coupling [8–11].

II. EXPERIMENTAL

High quality samples of Fe$_2$P have been synthesized using the drop synthesis method [12] and precharacterized with powder x-ray diffraction (XRD) and magnetometry. In-elastic neutron-scattering studies were performed using the cold chopper spectrometers of the Institute Laue Langevin and Heinz Maier-Leibnitz Zentrum (MLZ), IN5 [13], and TOFTOF [14]. Additionally, studies with Mössbauer spectroscopy (MS) were performed. The phonon and magnon spectra were calculated via first-principles simulations. Full details can be found in the Supplemental Material (SM [15]).

A. Elastic neutron scattering

X-ray diffraction determined a high purity sample with no detectable impurities. Mössbauer spectroscopy determined complete occupation of the two Fe sites. Susceptibility measurements indicate a ferromagnetic transition temperature $T_c = 220(2)$ K closely matched with information found in the literature, $T_c \approx 216$ K [8]. Mössbauer spectroscopy

---

*Corresponding author: johan.cedervall@kemi.uu.se
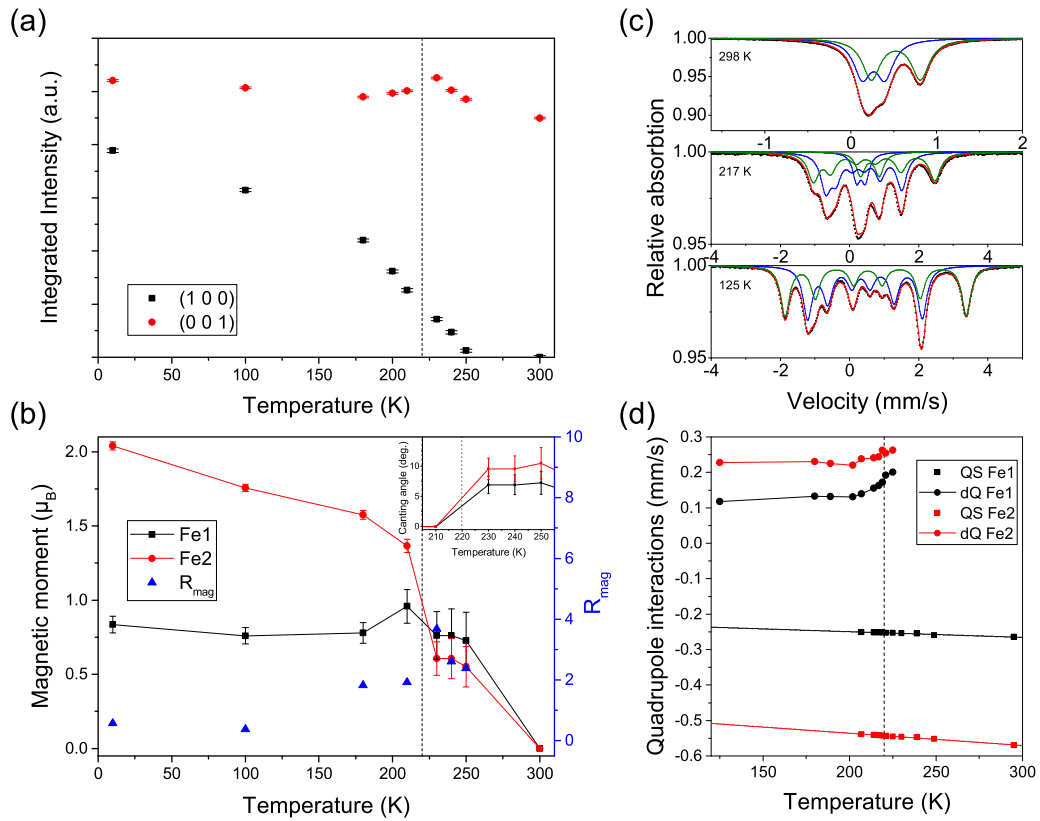†Corresponding author: pascale.deen@esss.se

FIG. 1. (a) Integrated intensity of the (1 0 0) and (0 0 1) peaks. For the (1 0 0) peak the structural contribution to the intensity from 300 K has been subtracted to emphasize the magnetic contribution. (b) Temperature dependence of the size of the magnetic moments. The R_{mag} values are shown in blue for each temperature. Inset shows the canting angle for temperatures above T_c. The dashed line indicates the Curie temperature for Fe_2P. (c) Representative Mössbauer spectra for Fe_2P in the three regions, paramagnetic (top), intermediate magnetic region (middle), and ferromagnetic region (bottom). (d) The electric quadrupole interactions QS and dQ for both Fe positions as function of temperature.

reveals a change in magnetic hyperfine fields for both Fe sites consistent with the FOMT with a transition region that is less than the experimental temperature resolution. The double differential neutron-scattering cross section has been measured for powdered Fe_2P across a range of temperatures, 10 K $< T <$ 300 K, and contains both static and dynamic magnetic and nuclear components. Previous work has indicated that the magnetic moments in Fe_2P align with the crystallographic c axis [9,10]. Magnetic neutron scattering is sensitive to the components perpendicular to the wave-vector transfer [16]. As such, the ferromagnetic contribution to the neutron-diffraction profile from Fe_2P is observed at a wave-vector transfer $Q = 1.2$ Å^{-1} corresponding to scattering from the [1 0 0] crystalline planes and magnetic moments aligned along the c axis. In contrast, scattering corresponding to the (0 0 1) Bragg peak at 1.8 Å^{-1} will be sensitive to nuclear contributions and magnetic moments perpendicular to the c axis. The static diffraction profiles were obtained by extracting the scattering corresponding to the elastic linewidth of the instruments. The magnetic moments in ferromagnetic Fe_2P, at 10 K, are aligned along the crystallographic c direction. A direct comparison of the integrated intensity of the (1 0 0) and (0 0 1) Bragg peaks, Fig. 1(a), reveals an increase in intensity of the (0 0 1) peak upon approaching T_c (220 K), which subsequently decreases upon heating to 300 K due to the effect of

the reduced Debye-Waller factor. A further detailed study of the magnetic structure (solved with the software SARAH [17]) was performed with the Rietveld method [18] implemented in FULLPROF [19]. The analysis revealed existing, but decreased, magnetic moments above T_c, canted from the c axis towards the a axis, Fig. 1(b), explaining the increased intensity of the (0 0 1) peak. The two ferromagnetic sites, Fe1 and Fe2, both show significant canting from the c direction with Fe1 rotating up to 7.6° and Fe2 significantly more, up to 11.6° at 250 K, inset in Fig. 1(b). These results are consistent with signatures from Mössbauer spectroscopy performed for Fe_2P in three regions, paramagnetic, ferromagnetic, and an intermediate region shown in Fig. 1(c). In Mössbauer spectroscopy, the first-order electric quadrupolar perturbation term dQ, for dominating magnetic interactions, clearly shows a variation, while the electric quadrupole splittings QS, show smooth variations close to T_c, further detail in SM [15]. These results are indicative of a rotation of the magnetic hyperfine fields away from the c axis close to T_c, Fig. 1(d).

B. Inelastic neutron scattering

Figure 2 shows the magnon and phonon excitations in Fe_2P at 100 and 200 K. Gapped acoustic phonons, $\Delta E = 0.54(8)$ meV are observed at 100 K around the wave-vector
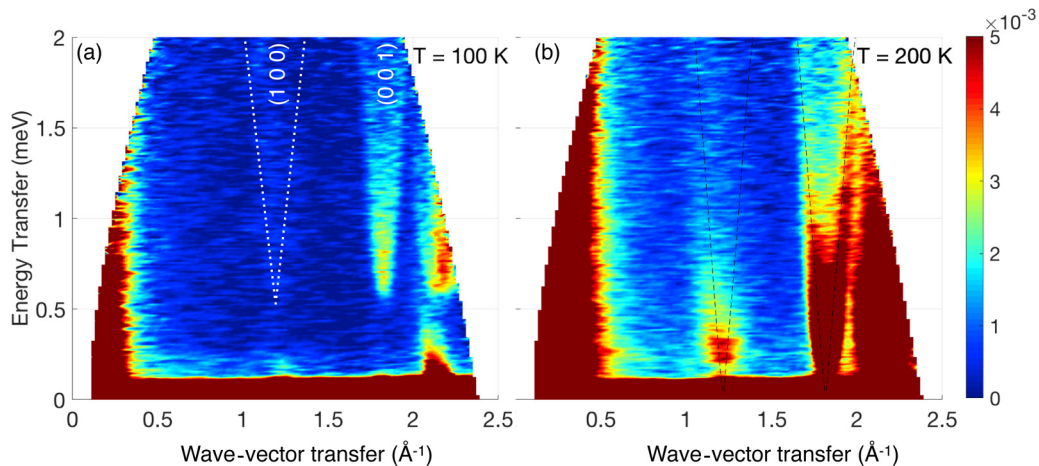
FIG. 2. $S(Q, \omega)$ ($E_i = 3.27$ meV) dependence at (a) 100 K, white dotted line indicates the phononic region around (1 0 0), (b) 200 K, the dashed linescorrespond to gapless phonons with E = DQ behavior (D = 12 meVÅ).

transfers for the orthogonal directions (1 0 0) and (0 0 1). At 200 K this gap has softened and can no longer be distinguished from the elastic line. The phonon stiffness at 100 K is 12.0(5) meV Å and shows minimal temperature dependence. The energy gap of the acoustic modes are strongly and linearly temperature dependent such that the energy gap is minimized around T_c, Fig. 3(a). Interestingly there is no anisotropy between the temperature dependence of the energy gap for the two orthogonal directions. A gap in the acoustic phonon is rather unusual but has previously been observed in spin-ladder compounds containing one-dimensional (1D) chains and two dimensional (2D) ladder substructures [20,21]. Gaps in the acoustic-phonon modes could be derived from sliding motions of one sublattice relative to the other with the precise gap value indicative of the strength of the Coulomb forces between the two charged sublattices [22]. An alternative explanation is that an energy gap in the acoustic-phonon mode is derived from boundary conditions as found from nanoclusters. Increased electron mobility, as a result of the gap in the phonon excitation, may enhance the magnetocaloric effect [23].

Neutron scattering from a nanostructured compound, such as found in 1D or 2D systems, would result in scattering at low wave-vector transfer and this is consistent with the scattering observed below 0.5 Å^{-1}, Fig. 3. Figure 3(b) shows the energy integrated intensity, -2 meV $< \Delta E < 2$ meV, of the scattering at low wave-vector transfer for 100 K $< T <$ 275 K. The low angle scattering is strongly temperature dependent and broadens in wave-vector transfer with increasing temperature, Fig. 3. The temperature dependence of this scattering indicates its magnetic origin. Below 200 K the short-range magnetic correlations are antiferromagnetic in origin as indicated by the positive gradient of the scattering profile. At 200 K the magnetic scattering profile is almost Q independent and above 220 K significant short-range ferromagnetic correlations develop. The profile of these excitations can be subdivided into two regions, below and above $Q = 0.59$ Å^{-1}. Below $Q = 0.59$ Å^{-1} the correlations can be described by a linear fit across all temperatures. For $Q > 0.59$ Å^{-1} the data do not conform to a simple curve or linear feature. These

features indicate that there are several length scales present in the short-range order consistent with complex nanostructures. The nanoscale structures are antiferromagnetically coupled below T_c with ferromagnetic coupling above T_c. A more detailed investigation using small angle neutron scattering is required to understand the finer details of these magnetic interactions and structures.

Magnetic excitations are evidenced when integrating in wave vector transfer across (1 0 0) and (0 0 1). Figure 3(c) shows two low-lying excitations, measured at 100 K, at 0.238(8) and 0.441(4) meV respectively, that exist for (1 0 0), Fig. 3(c), but not for (0 0 1), Fig. 3(d), and can therefore be ascribed to magnetic excitations. At 200 K the phonon excitations have softened to such an extent that they overlap in energy and wave-vector transfer with the magnetic excitations, Fig. 3(e). The phonons seen in Fig. 4(f) show the same trend as in (e) without any interplay from the magnon excitations. As such the phonons and magnons have hybridized to produce magnon-phonon quasiparticles. There is therefore a strong indication that magnon-phonon coupling is present at the FOMT in Fe$_2$P.

III. FIRST PRINCIPLES CALCULATIONS

Figure 4(a) presents the phonon band structure along high-symmetry lines in the hexagonal Brillouin zone of Fe$_2$P obtained from *ab initio* simulations (see SM for further details [15]). All phonon frequencies are positive suggesting that the hexagonal crystal structure is stable. Two out of three acoustic modes are degenerate (as expected for hexagonal structure). The acoustic branches are linear as $Q \rightarrow 0$, and the transverse modes have a quadratic dispersion near the Γ point. Some interplay is visible between the acoustic modes as well as the transverse/optical modes. The layer-layer interaction along the c direction [0 0 1] is not negligible as seen from the band structure along Γ-A, L-M, K-H. The experimental results at low temperatures match the theoretical expectation considering the phonon stiffness. However, the calculated phonon band structure is not gapped since the macroscopic crystalline structure is not taken into account. Current
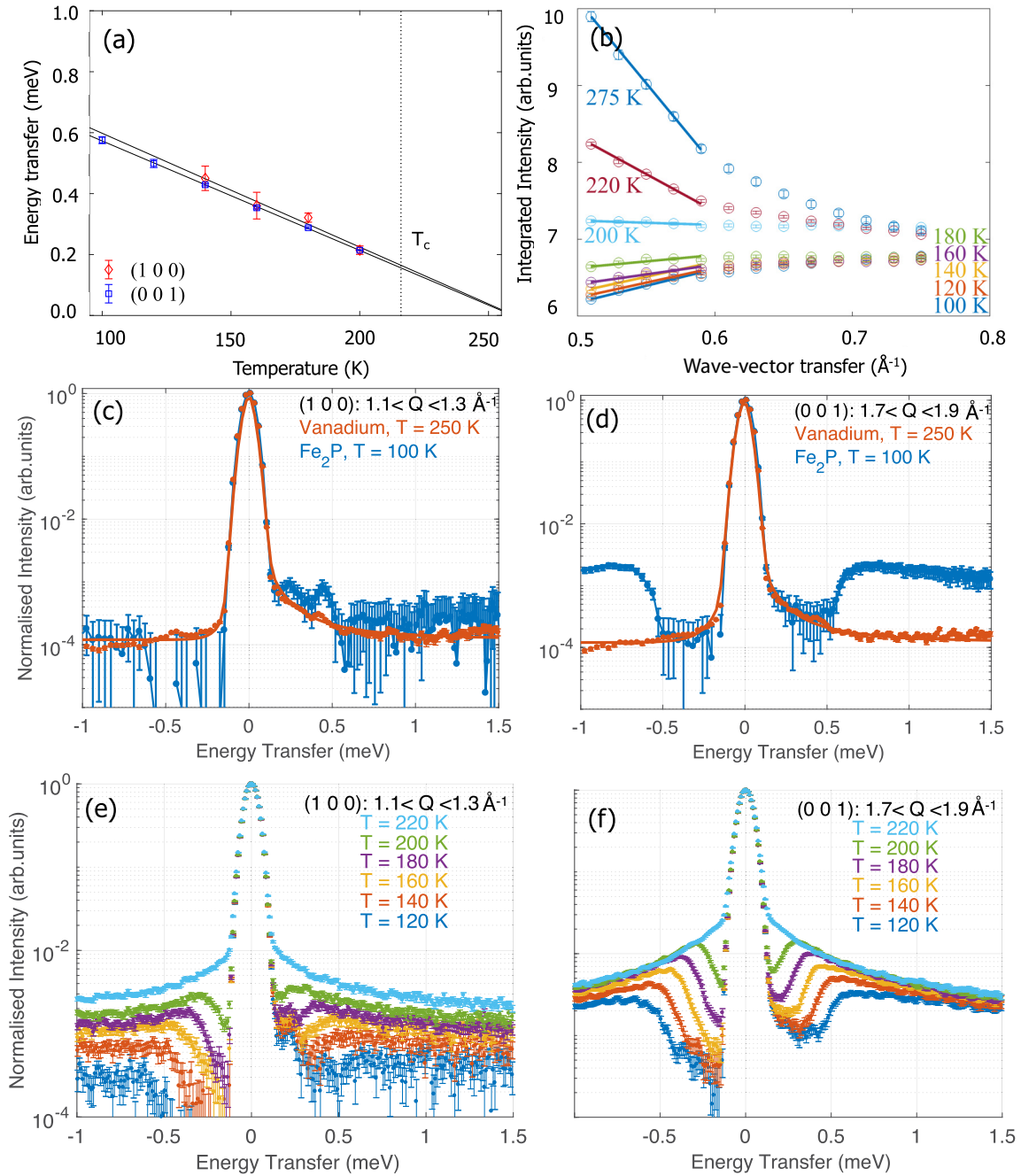
FIG. 3. (a) Temperature dependence of the phonon gap for (1 0 0) and (0 0 1). (b) Scattering at low wave-vector transfer integrated across $-2 < E < 2$ meV. (c) Low-lying excitations at 100 K across (1 0 0), integrated across $1.1 < Q < 1.3$ Å^{-1} and (d) (0 0 1) integrated across $1.7 < Q < 1.9$ Å^{-1}, the instrumental resolution is described by the vanadium scattering juxtaposed on the figure. (e) Temperature dependence of the low-lying excitations around (1 0 0) and (f) (0 0 1).

theoretical analysis can not take into account the macroscopic crystalline structure and we hope these results will stimulate further theoretical analysis in this direction.

A direct comparison can be made between the theoretical expectation and the experimental results at 200 K at which point the energy gap is minimal, Fig. 2(b). A slight broadening of the linewidth and phonon stiffness is expected considering that the experimental results are obtained at 200 K,

while theoretical results are for $T = 0$ K. It seems, however, that the theoretical calculations overestimate the measured phonon stiffness, 35 meV Å, compared to the experimental 12.0(5) meV Å.

The theoretical magnetic moments were calculated to 1.367 μ_B and 2.177 μ_B for Fe1 and Fe2, respectively, in good agreement with the measured data. The nearest-neighbor exchange interactions are $J_{ij}^{Fe1-Fe1} = 11.2$ meV, $J_{ij}^{Fe1-Fe2} =$
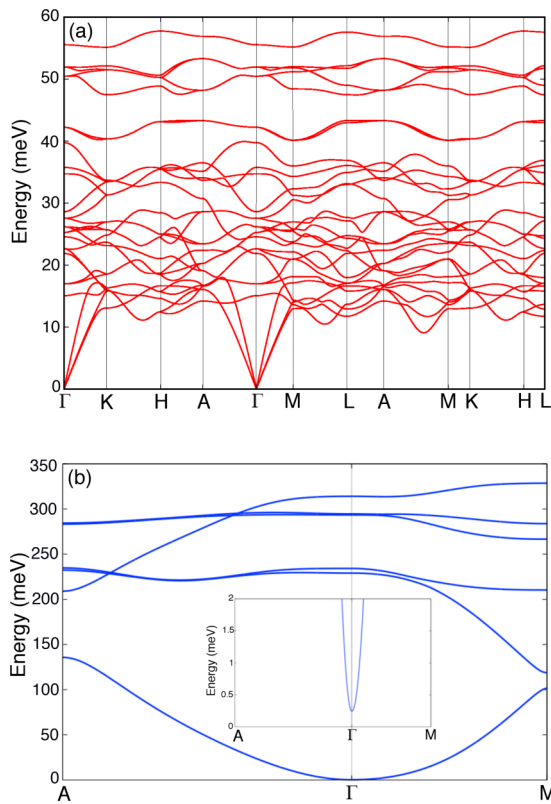
FIG. 4. (a) Phonon band structure of ferromagnetic Fe$_2$P. (b) Adiabatic magnon spectra calculated for Fe$_2$P using linear spin-wave theory. The inset shows a zoom around the Γ point in order to show the spin gap induced mainly by the uniaxial anisotropy.

8.4 meV and $J_{ij}^{\text{Fe2}-\text{Fe2}} = 14.7$ meV. The Dzyaloshinskii-Moriya (DM) interactions were found to be of the order of μeV. The adiabatic magnon spectrum, in Fig. 4(b), was found to have a spin gap at the Γ point [inset in Fig. 4(b)]. The gap is theoretically quantified to 0.26 meV and is a result of the spin-orbit coupling which induces the DM interaction and the uniaxial anisotropy [24]. Since the DM interaction is very small, the influence on the spin gap is very small, around 0.01% of the total gap. In consequence, the spin gap is largely driven by uniaxial anisotropy. Even though the calculations were performed at 0 K, the spin gap obtained by calculating the magnon spectra is of similar magnitude as the experimental gap [0.238(8) meV] shown in Fig. 3(c). There is

no indication of a second magnetic excitation in the theoretical results as observed in neutron inelastic scattering.

IV. CONCLUSIONS

In conclusion, the interplay between magnetic and phonon degrees of freedom in the magnetocaloric compound Fe$_2$P has been probed with the aim to determine the mechanism that leads to the FOMT, considered crucial for the MC effect. Neutron diffraction and Mössbauer spectroscopy shows that the magnetic moments cant slightly from the nominal c axis close to T_c. Inelastic neutron scattering show gapped acoustic phonon modes for $T < T_c$, consistent with nanoscale clusters that are weakly antiferromagnetically correlated below T_c and develop into ferromagnetic nanoclusters above T_c. Usually, phonons limit both spin-relaxation times and electron mobility in solids, yet a gapped acoustic-phonon mode would give rise to enhanced electron mobility that may aid the magnetocaloric effect. The phonon gap is strongly temperature dependent and hybridizes with the magnon excitations at 0.238(8) and 0.441(4) meV for $T \sim T_c$, consistent with canting of the magnetic moments. First-principles calculations reveal that the expected phonon spectrum width, and thus that the phonon stiffness, is consistent with the experimental results. However, the theory provides no energy gap in the phonon excitations for $T < T_c$ and thus must be reconsidered in light of these results. Theoretical investigation of magnetic properties are able to determine that the low-lying magnetic excitations 0.238(8) meV originates from the uniaxial anisotropy, yet does not reveal the second magnetic excitation probed by neutron inelastic scattering. These results shed significant light on the magnetothermodynamic phenomena and should give rise to further experimental and theoretical studies.

[1] E. França, A. dos Santos, A. Coelho, and L. da Silva, J. Magn. Magn. Mater. **401**, 1088 (2016).

[2] E. Brück, J. Phys. D **38**, R381 (2005).

[3] V. V. Khovaylo, V. V. Rodionova, S. N. Shevyrtalov, and V. Novosad, Phys. Status Solidi B **251**, 2104 (2014).

[4] K. A. Gschneidner, Jr. and V. K. Pecharsky, Int. J. Refrig. **31**, 945 (2008).

[5] E. Warburg, Ann. Phys. **249**, 141 (1881).

[6] K. A. Gschneidner, Jr. and V. K. Pecharsky, Annu. Rev. Mater. Sci. **30**, 387 (2000).

[7] R. Gauß, G. Homm, and O. Gutfleisch, J. Ind. Ecol. **21**, 1291 (2016).

[8] L. Lundgren, G. Tarmohamed, O. Beckman, B. Carlsson, and S. Rundqvist, Phys. Scr. **17**, 39 (1978).

[9] D. Scheerlinck and E. Legrand, Solid State Commun. **25**, 181 (1978).

[10] H. Fujii, S. Komura, T. Takeda, T. Okamoto, Y. Ito, and J. Akimitsu, J. Phys. Soc. Jpn. **46**, 1616 (1979).

[11] S. Komura, K. Tajima, H. Fujii, Y. Ishikawa, and T. Okamoto, J. Magn. Magn. Mater. **15**, 351 (1980).

[12] B. Carlsson, M. Gölin, and S. Rundqvist, J. Solid State Chem. **8**, 57 (1973).

[13] P. P. Deen, M. S. Andersson, J. Cedervall, H. Mutka, P. Nordblad, and M. Sahlberg, *Interplay between Phonon and Magnon Excitations in the Magnetocaloric Fe$_2$P Based Alloys* (2016), https://doi.ill.fr/10.5291/ILL-DATA.7-01-441.

[14] H. M.-L. Zentrum, W. Lohstroh, and Z. Evenson, J. Large-scale Res. Facil. **1**, A15 (2015).

[15] See Supplemental Material at http://link.aps.org/supplemental/10.1103/PhysRevB.99.174437 for description of the synthesis and computational methods, as well as details for the XRD, magnetometry, and Mössbauer spectroscopy analysis, which includes Refs. [9,12,25–36].

[16] G. L. Squires, *Introduction to the Theory of Thermal Neutron Scattering*, 3rd ed. (Cambridge University Press, Cambridge, 2012).

[17] A. Wills, Physica B **276-278**, 680 (2000).

[18] H. M. Rietveld, J. Appl. Crystallogr. **2**, 65 (1969).

[19] J. Rodríguez-Carvajal, Physica B **192**, 55 (1993).

[20] V. K. Thorsmølle, C. C. Homes, A. Gozar, G. Blumberg, J. L. M. van Mechelen, A. B. Kuzmenko, S. Vanishri, C. Marin, and H. M. Rønnow, Phys. Rev. Lett. **108**, 217401 (2012).

[21] X. Chen, D. Bansal, S. Sullivan, D. L. Abernathy, A. A. Aczel, J. Zhou, O. Delaire, and L. Shi, Phys. Rev. B **94**, 134309 (2016).

[22] G. Theodorou, Solid State Commun. **33**, 561 (1980).

[23] M. Droth and G. Burkard, Phys. Rev. B **84**, 155404 (2011).

[24] M. Costa, O. Grånäs, A. Bergman, P. Venezuela, P. Nordblad, M. Klintenberg, and O. Eriksson, Phys. Rev. B **86**, 085125 (2012).

[25] T. J. B. Holland and S. A. T. Redfern, Mineral. Mag. **61**, 65 (1997).

[26] L. Caron, M. Hudl, V. Höglin, N. H. Dung, C. P. Gomez, M. Sahlberg, E. Brück, Y. Andersson, and P. Nordblad, Phys. Rev. B **88**, 094440 (2013).

[27] G. Kresse and J. Furthmüller, Phys. Rev. B **54**, 11169 (1996).

[28] J. P. Perdew, K. Burke, and M. Ernzerhof, Phys. Rev. Lett. **78**, 1396 (1997).

[29] A. Togo, F. Oba, and I. Tanaka, Phys. Rev. B **78**, 134106 (2008).

[30] B. Skubic, J. Hellsvik, L. Nordström, and O. Eriksson, J. Phys.: Condens. Matter **20**, 315203 (2008).

[31] A. I. Liechtenstein, M. I. Katsnelson, and V. A. Gubanov, J. Phys. F **14**, L125 (1984).

[32] A. Liechtenstein, M. Katsnelson, V. Antropov, and V. Gubanov, J. Magn. Magn. Mater. **67**, 65 (1987).

[33] H. Ebert, D. Ködderitzsch, and J. Minár, Rep. Prog. Phys. **74**, 096501 (2011).

[34] T. Ericsson, L. Häggström, R. Wäppling, and T. Methasiri, Phys. Scr. **21**, 212 (1980).

[35] R. Wäppling, L. Häggström, T. Ericsson, S. Devanarayanan, E. Karlsson, B. Carlsson, and S. Rundqvist, Journal of Solid State Chemistry France **13**, 258 (1975).

[36] H. Fujii, Y. Uwatoko, K. Motoya, Y. Ito, and T. Okamoto, J. Phys. Soc. Jpn. **57**, 2143 (1988).